Toll like receptors TLR1/2, TLR6 and MUC5B as binding interaction partners with cytostatic proline rich polypeptide 1 in human chondrosarcoma

KARINA GALOIAN[1], SILVA ABRAHAMYAN[2], GOR CHAILYAN[2], AMIR QURESHI[1], PARTHIK PATEL[1],
GIL METSER[1], ALEXANDRA MORAN[1], INESA SAHAKYAN[2], NARINE TUMASYAN[2], ALBERT LEE[2],
TIGRAN DAVTYAN[3], SAMVEL CHAILYAN[2] and ARMEN GALOYAN[2*]

[1]Department of Orthopedic Surgery, University of Miami Miller School of Medicine, Miami, FL, USA; [2]Buniatian Institute
of Biochemistry Academy of Sciences of Armenia, Yerevan 0014; [3]Analytical Laboratory Branch of E. Gabriyelian
Scientific Center of Drug and Medical Technology Expertise of Ministry Health of Armenia, Yerevan 0002, Armenia

Abstract. Metastatic chondrosarcoma is a bone malignancy not responsive to conventional therapies; new approaches and therapies are urgently needed. We have previously reported that mTORC1 inhibitor, antitumorigenic cytostatic proline rich polypeptide 1 (PRP-1), galarmin caused a significant upregulation of tumor suppressors including TET1/2 and SOCS3 (known to be involved in inflammatory processes), downregulation of oncoproteins and embryonic stem cell marker miR-302C and its targets Nanog, c-Myc and Bmi-1 in human chondrosarcoma. To understand better the mechanism of PRP-1 action it was very important to identify the receptor it binds to. Nuclear pathway receptor and GPCR assays indicated that PRP-1 receptors are not G protein coupled, neither do they belong to family of nuclear or orphan receptors. In the present study, we have demonstrated that PRP-1 binding interacting partners belong to innate immunity pattern recognition toll like receptors TLR1/2 and TLR6 and gel forming secreted mucin MUC5B. MUC5B was identified as PRP-1 receptor in human chondrosarcoma JJ012 cell line using Ligand-receptor capture technology. Toll like receptors TLR1/2 and TLR6 were identified as binding interaction partners with PRP-1 by western blot analysis in human chondrosarcoma JJ012 cell line lysates. Immunocytochemistry experiments confirmed the finding and indicated the localization of PRP-1 receptors in the tumor nucleus predominantly. TLR1/2, TLR6 and MUC5B were downregulated in human chondrosarcoma and upregulated in dose-response manner upon PRP-1 treatment. Experimental data indicated that in this cellular context the mentioned receptors had tumor suppressive function.

Correspondence to: Professor Karina Galoian, Department of Orthopedic Surgery, University of Miami Miller School of Medicine, 1600 NW 10th Avenue 1140, Miami, FL 33136, USA
E-mail: kgaloian@med.miami.edu

*Deceased

Introduction

Chondrosarcoma is cancer of the cartilage that eventually metastasize. The disease can affect multiple organs, such as long bones, spine, pelvis, larynx and head. Conventional therapies are not effective in this disease treatment and there is urgency in seeking new approaches (1,2). The signaling events resulting in mesenchymal cell transformation to sarcoma have yet to be fully elucidated. Proline rich polypeptide 1, (PRP-1), also known as (galarmin) is produced by the brain neurosecretory cells and comprised of 15 amino acids (3), and is a mTOR kinase (mTORC1) inhibitor in chondrosarcoma, which causes 80-90% inhibition of chondrosarcoma cell growth, halting G1/S phase cell cycle progression in chondrosarcoma (4,5) and other mesenchymal tumors (6). The ability of PRP-1 to upregulate tumor suppressor miRNAs and downregulate onco-miRNAs in human chondrosarcoma JJ012 cell line was demonstrated (7). The upregulation of most tumor suppressors in chondrosarcoma (8) including inflammation related TET1/2 and SOCS3 is one of the unique PRP-1 properties, however, it depends on which molecular pathway these tumor suppressors are part of (9). PRP-1 epigenetically downregulates embryonic stem cell marker miR-302c in human chondrosarcoma and its targets Nanog, c-Myc and Bmi1 (10). To understand better the mechanism of PRP-1 action and its potential as therapeutic agent in the future, it is very important to identify the receptor it binds to. In the present study, we present evidence that PRP-1 exerts its effect via interacting with toll like receptor family TLR1/2, TLR6 and mucin MUC5B. Innate immunity toll-like receptors (TLRs), or pattern recognition receptors are sensitive both to endogenous and exogenous ligands (11,12) and can be found both inside the cells and at the cell surface. Intracellular TLRs start their journey from the endoplasmic reticulum (ER) through the Golgi and eventually to endolysosomes (13). TLRs

play active roles in carcinogenesis and tumor progression or its inhibition (14,15) where the activation of TLR signalling could regulate antitumor immunity of the host (16). The term alarmins is often used when referring to endogenous TLR ligands. The innate immune system can be activated by recognizing pathogen associated molecular patterns (PAMPs). The injured cells in their turn have ability to release danger-associated molecular patterns (DAMPs) and contribute to the activation of innate immune system. Thus, immune system is involved not only in fighting the infection by mobilizing the immunologic arsenal, but also in the process of tissue repair. Hence, the term non-infectious inflammation response, whenever TLR signaling is mediated by endogenous ligands, which secure autoimmune disease and tumorigenesis in addition to tissue repair and injury (17,18). TLRs1 (cluster of differentiation 281), 2, 4, 5 and 6 are expressed on the cell surface, whereas TLRs3, 7, 8 and 9 are intracellular nucleic acid receptors. The ligand for TLR10 remains to be found (19). The antitumorigenic role of TLR2 is recognized, its deficiency led to early intestinal tumor formation (20). Most of endogenous TLR ligands are agonists of TLR4 and TLR2 (21). There is a reported link berween TLR signaling andmucins (MUCs) leading to effective pathogen elimination (22-24). Mucins are glycosylated large extracellular proteins that are found not only in mucous cells but also in connective tissue and goblet cells. Mucin expression glycosylation alterations can lead to the development of cancer and cellular transformation (25-31). Apomucin with the attached O-linked oligosaccharides is the protein backbone for mucin. There are 'secreted (gel-forming and non-gel-forming)' and 'membrane-bound' mucins, with transmemebrane domain (32). The goblet cells from the epithelium and mucous cells from submucosal glands generate secreted mucins. Secreted mucins on the chromosome 11p15 include MUC2, MUC5AC, MUC5B, MUC6 and MUC19. Some of the mucins can manifest themselves as tumor suppressors, for example MUC4 (33,34). MUC5B expression has protumorigenic (28,35) or antitumorigenic consequence for the cell growth (36,37) and was linked both to decreased survival or better prognosis in cancer patients correspondingly, depending on the disease and organ specificity. MUC5B was shown to have very beneficial effects in human airway defense (38). The epigenetic mechanism, hypermethylation of MUC5B promoter was attributed to the silencing of its tumor suppressor activity (39). Both overexpression and downregulation of mucins in different organs can contribute to cancer pathology and inflammation (26,40).

Materials and methods

PRP-1 initial isolation and chemical synthesis. Initially, PRP-1 was isolated from the neurosecretory granules of bovine neurohypophysis by the method described (3,41) followed by its chemical synthesis (42).

PRP-1 antiserum affinity chromatography purification. Antiserum for PRP1 was generated (43), then affinity chromatography purified, AminoLink Plus Immobilization kit instructions (44894; Thermo Fisher Scientific, Waltham, MA, USA) were followed for protein sample desalting with Zeba Spin columns (89891; Thermo Fisher Scientific).

Tissue culture. The human JJ012 chondrosarcoma cell line was received from Dr Joel Block's Laboratory (Rush University, Chicago IL, USA). JJ012 chondrosarcoma cells were cultured as previously described (8). The medium composition: Dulbecco's modified Eagle's medium (DMEM), supplemented with F12, 10% fetal bovine serum (FBS), 25 μg/ml ascorbic acid, 100 ng/ml insulin, 100 nM hydrocortisone and 1% penicillin/streptomycin.

Brief immunocytochemistry protocol. Adherent cells were grown directly on coverslips with $5x10^5$ cells/coverslip in 6-well clusters, where they were cultured overnight at 37°C in an incubator. Twenty-four hours later the medium was removed and samples were fixed in 1 ml of 4% formaldehyde solution, (F8775; Sigma-Aldrich St. Louis, MO, USA) in phosphate-buffered saline (PBS), pH 7.4 1X Gibco, (10010-023) PBS for 15 min in the incubator. Samples were washed with PBS twice, then were permeabilized with PBS/Triton X-100 (T9284; Sigma-Aldrich), 1% for 5 min at room temperature. Detergent was removed and non-specific sites were blocked in PBS containing 2% bovine serum albumin (BSA, A2153; Sigma-Aldrich) at room temperature for 30 min. Samples were further incubated overnight in cold room along with all primary antibodies for the experiment, followed by two consecutive washes the next morning and incubation in BSA solution with secondary antibodies at room temperature for 2 h along with Zenon complex and two washes with PBS, for 10 min each. Second fixation step with formaldehyde for 15 min at room temperature in the dark was performed, followed by two washing steps.

Zenon complex formation. PRP-1 serum antibody and Zenon rabbit IgG, Alexa Fluor 488 (Z-25302; Molecular Probes, Eugene, OR, USA) were mixed according to the manual and the procedures. The mixture was incubated for 10 min at room temperature with labeling reagent A, then another 10 min incubation with the blocking reagent B and 1 ml of the resulting mixture was applied to each well. Cells were stained with 3 μM of 4',6-diamino-2-phenylindole dihydrochloride (DAPI, D1306; Thermo Fisher Scientific) for nuclear staining or 10 min at room temperature, the washed with PBS twice. The samples on coverslips were mounted in Antifade mounting medium, followed by microscopy. ProLong Gold Antifade reagent (P10144; Life Technologies) was applied as a liquid mountant directly to fluorescently labeled cells on microscope slides. The reagent contains chemicals to protect fluorescent dyes from fading during fluorescence microscopy.

Antibodies used for immunocytochemistry. For plasma membrane staining wheat germ agglutinin Alexa Fluor 594 conjugate was used (W11262; Thermo Fisher Scientific); TLR1 rabbit antibody (ab180798; Abcam); goat anti-rabbit H&L (DyLight 550) (ab96884; Abcam); mouse anti-MUC5B, Abcam (ab77995); goat anti-mouse IgG secondary antibody Alexa Fluor 647 (A2124; Life Technologies).

Imaging. Image acquisition was performed by the Analytical Imaging Core Facility at DRI/SCCC, University of Miami (FL, USA).

Zeiss 200M, ApoTome fluorescent microscope, DAPI 49, GFP 38HE, Cy3 43, Cy5 50 filter cubes, heated stage, Orca II ERG Hamamatsu b/w 14 bit camera and AxioVision acquisition software were used. The coverslips were placed in regular 35-mm Petri dishes and the cells grown on them, covered with medium. Once the cells were grown, the coverslips were taken out, the cells were fixed, stained and mounted on the glass slides. For imaging controls secondary antibodies were used without the primaries.

Human MUC5B ELISA and electrophoresis and western blotting. MUC5B protein was measured with human mucin -5 subtype (MUC5B) ELISA kit (MyBioSource, San Diego, CA, USA) (MBS 704534-48T).

The cells were trypsinized once they reached confluency and then seeded in 6-well clusters at a concentration of $1x10^6$ cells/ml. PRP-1 was added only to the experimental samples but not to controls. The overnight incubation in 5% CO_2 incubator at 37°C was followed by cell wash with ice-cold PBS with added protease inhibitor. The cell lysis buffer (C2978; Sigma-Aldrich) was supplemented with the protease inhibitor in a 1:100 ratio. The cells were collected with a scraper and centrifuged at 15,000 x g at 4°C. The supernatant was collected and the protein concentration was measured. The pellets were frozen at -80°C until loading on the gel (20 μg/lane). Polyacrylamide gel electrophoresis and western blotting reagents were supplied by Lonza, Inc. (Allendale, NJ, USA), and all the related procedures followed the company's protocol. The catalog numbers for the reagents and the suppliers are listed below for convenience, although they were reported in our previous communication (8). PAGEr™ Gold Precast Gels (59502; 10% Tris-Glycine; Lonza); ECL reagent (RPN2109; GE Healthcare, Little Chalfont, UK); Western Blocker solution (W0138; Sigma-Aldrich); ProSieve QuadColor Protein marker (4.6-300 kDa, 00193837; Lonza); 20X Reducing Agent for ProSieve ProTrack Dual Color Loading buffer (00193861; Lonza); ProTrack Loading buffer (00193861; Lonza); ProSieve ProTrack Dual Color Loading buffer EX running buffer (00200307; Lonza); ProSieve EX Western Blot Transfer buffer (00200309; Lonza); Immobilon®-P PVDF Membranes (P4188; Sigma-Aldrich).

Immunoblot antibodies. Rabbit polyclonal anti-TLR6 (ab37072), MW 92 kDa (Abcam); rabbit anti-TLR1 cell (2209), MW 86 kDa (Cell Signaling Technology, Danvers, MA, USA); rabbit anti-TLR1 (ab68158), MW 90 kDa (Abcam); mouse anti-TLR2 [TL2.1], (ab9100), MW 90 kDa (Abcam); Mouse anti-TLR3 (TLR3.7) (sc-32232), MW 104 kDa (Santa Cruz Biotechnology, Santa Cruz, CA, USA); mouse anti-TLR4 (25) (sc-293072), MW 95-120 kDa (Santa Cruz Biotechnology); mouse anti-TLR5 (19D759.2), (sc-57461), MW 110-120 kDa (Santa Cruz Biotechnology); rabbit anti-TLR7, (5632), MW 140 kDa (Cell Signaling Technology); mouse TLR 8 (9A6), (sc-135584), MW 119.8 kDa (Santa Cruz Biotechnology); rabbit anti-TLR9, (5845), MW 130 kDa (Cell Signaling Technology); mouse TLR10 (2A11), sc-293300, MW 90 kDa (Santa Cruz Biotechnology); mouse anti-tubulin, (T5168; Sigma-Aldrich); rabbit anti-TRIF/TICAM1, NBP2-31189, MW 75 kDa (Novus Biologicals, Littleton, CO, USA); mouse anti-TICAM2, MW 21 kDa (Santa Cruz Biotechnology);

rabbit anti-TRAF6 (3566R-100), MW 54 kDa (BioVision, Inc., Milpitas, CA, USA); goat anti-rabbit IgG, HRP-linked (7074; Cell Signaling Technology); anti-mouse IgG, HRP-linked (7076; Cell Signaling Technology).

Lead Hunter discovery services (DiscoveRx). Nuclear Hormone Receptor Assays: PathHunter® NHR Protein Interaction (Pro) and Nuclear Translocation (NT) assays monitor the activation of a nuclear hormone receptor in a homogeneous, non-imaging assay format using a technology developed by DiscoveRx called enzyme fragment complementation (EFC). The company described NHR Pro assay detects of protein-protein interactions between an actvated NHR protein and a nuclear fusion protein containing steroid receptor co-activator peptide (SRCP). When bound by ligand, the NHR will migrate to the nucleus and recruit the SRCP domain, whereby complementation occurs, generating a unit of active β-galactosidase (β-gal) and production of chemiluminescent signal.

Arrestin pathway: The PathHunter® β-arrestin assay based on activation of a GPCR using a method developed by DiscoveRx called enzyme fragment complementation (EFC) with β-galactosidase (β-gal) as the functional reporter (44). In brief, according to the manufacturer's protocol: the enzyme is split into two inactive complementary portions (EA for enzyme acceptor and ED for enzyme donor) expressed as fusion proteins in the cell. EA is fused to β-arrestin and ED is fused to the GPCR of interest. When the GPCR is activated and β-arrestin is recruited to the receptor, ED and EA complementation occurs, restoring β-gal activity which is measured using chemiluminescent PathHunter® detection reagents.

Data analysis. The GPCR max panel % agonist was calculated as 100% (mean of test samples - mean of vehicle control)/mean Max control ligand - mean of vehicle control). For antagonist mode assays, percentage inhibition was calculated using the following formula: % Inhibition =100% x (1 - (mean RLU of test sample - mean RLU of vehicle control)/(mean RLU of EC80 control - mean RLU of vehicle control). For the orphan max panel, % agonist activity was calculated as 100% x (mean of test sample - mean of vehicle control)/mean of vehicle control.

gpcrMAX and NHR - Agonist mode calculation: To determine if a compound is potentially acting as an agonist to activate the receptor and induce arrestin recruitment the following factors should be considered: Is the % activity >30%? If so, is the compound mean RLU >Baseline RLU + 3 x Baseline SD.

gpcrMAX and NHR - Antagonist mode: Inhibition of GPCR activation by a compound acting as an antagonist of ligand binding results in a decrease in β-arrestin recruitment to the target GPCR. The NHR panel measures agonist interactions during a 6-h period and antagonist are preincubated for 1 h prior to agonist challenge. To determine if a compound is potentially acting as an antagonist to inhibit receptor activation the following factors should be considered: Is the % inhibition >35%, if so, is the compound mean RLU <EC80 RLU - 3 x EC80 SD.

orphanMAX - Agonist mode: Activation of Orphan GPCR by a compound acting as an agonist will result in an increase in β-arrestin recruitment to the target orphan GPCR. To determine if a compound is potentially acting as an agonist

to activate an orphan receptor and induce arrestin recruitment the following factor should be considered: Is the % activity >50%. If so, is the compound mean RLU >Baseline RLU + 3 x Baseline SD.

TriCEPS technology. This technology from Dualsystems Biotech AG (Zurich, Switzerland) was implemented to detect PRP-1 receptor or interacting partners. Specific cell surface protein receptors are involved in the drug, peptide ligand mediated physiological responses. The TriCEPS method is based on the Ligand-based receptor capture (LRC) technology where special reagent can be coupled to a ligand of interest, which allows to capture the ligand when bound to corresponding receptors. One can picture TriCEPS with three arms: one that binds to amino group containing ligands, a second for the ligand-based capture of glycosylated and a third one with biotin tag for purifying receptor peptides to be analyzed by quantitative mass spectrometry (MS). Specific receptors for the ligand of interest are identified through quantitative comparison of the identified peptides with a sample generated by a control probe with known (e.g., insulin) receptor.

TriCEPS protocol: Ligand coupling: This procedure implemented processing of ligand and the identification of receptor candidates (3 ligand and 3 control samples, 300 μg control ligand or 300 μg ligand of interest to 120 μl of 25 mM HEPES pH 8.2, 1.5 μl (150 μg) TriCEPS v.3 was added to both reactions and mixed immediately by pipetting up and down using a 200 μl pipette, then incubated at 20°C under gentle agitation (350 rpm) in a ThermoMixer for 90 min. Cell preparation and oxidation 1.2x10^8 cells were utilized for the experiment in triplicates. Cells were centrifuged at 300 x g for 5 min at 4°C, then were resuspended in 49 ml LRC buffer. The oxidation agent 1 ml (75 mM sodium metaperiodate) were added to a final concentration of 1.5 mM metaperiodate, followed by incubation for 15 min at 4°C. The mild oxidant sodium metaperiodate generates aldehydes from carbohydrates that link to the proteins of cell surface. When the ligand binds to the receptor, the hydrazine group formed a bond with the aldehyde for protein labeling.

Mass spectrometry. The LRC-TriCEPS samples were analyzed on a Thermo LTQ Orbitrap XL spectrometer. The samples were processed in data dependent acquisition mode in a 90-min gradient with 10 cm C18 packed column. The statistical ANOVA model was applied to the six remaining samples in the CaptiRec dataset. With models of Gaussian distribution the system tests each protein for differential abundance in all pairwise comparisons of ligand and control samples and calculates P-values. P-values are undergoing multiple comparisons to control the experiment-wide false discovery rate (FDR). Then, this adjusted P-value from each individual protein is plotted against the magnitude of the fold enrichment between the two experimental conditions. The receptor candidate space is defined based on the criteria where the area in the volcano plot that is limited by an enrichment factor of ≥4-fold and an FDR-adjusted P≤0.01.

RT2 qPCR primer assays. These custom designed assays by Qiagen (Valencia, CA, USA) served as sensitive gene expression profiling tool for real-time PCR analyses. Assay utilized RT2 SYBR-Green qPCR Master Mixes. Mature RNA isolated using RNA extraction according to the manufacturer's instructions. RNA quality was determined using a spectrophotometer and was reverse transcribed using a cDNA conversion. The cDNA in combination with RT2 SYBR-Green qPCR Master Mix (cat. no. 330529) was used with RT2 qPCR assays. Ct values were uploaded on web portal at http:// www.qiagen.com/geneglobe. Samples were assigned to control and test groups. Ct values were normalized based on a manual selection of reference genes. The data analysis web portal calculates fold change/regulation using ΔΔCt method, in which ΔCt is calculated between gene of interest (GOI) and an average of housekeeping genes (HKG) followed by ΔΔCt calculations [ΔCt(experiment) - ΔCt(control)]. Fold change is then calculated using the $2^{-\Delta\Delta Ct}$ formula.

Results

PRP-1 receptors are not G protein coupled, neither nuclear nor orphan receptors. The search for PRP-1 binding partners started with DiscoverX platform of G protein coupled receptors, (GPCR) in agonist, (Table I) and antagonist modes (Table II). There was no indication that PRP-1 was G protein coupled, neither that this peptide was agonist for orphan receptors (Table III) or agonist/antagonist for nuclear receptor in nhrMax panels (Table IV). MUC5B was identified as PRP-1 receptor binding partner in human chondrosarcoma JJ012 cell line using Ligand-receptor capture technology. We proceeded further in the attempt to identify binding partners for PRP-1 using TriCEPS Ligand-receptor capture (LRC) technology from Dualsystems Biotech AG (45). LRC was used to identify novel ligand-receptor interactions. After the TriCEPS coupled ligand (PRP-1) bound to its targets in or at the cell membrane the second arm of TriCEPS coupled to the glycans of that target receptor. The third arm of TriCEPS was used to isolate the proteins that are bound to TriCEPS (Fig. 1A). In the next step the isolated proteins were subjected to a trypsin digest. The resulting peptides of the digest were identified and quantified using liquid chromatography, tandem mass spectrometry (LC-MS/MS) (45,46). Then, the quantified peptides from the control reaction (transferrin as ligand) were compared to the ligand of interest (PRP-1) reaction (labelled in the volcano plot as peptide). The proteins that were 4-fold enriched in one of the treatments compared to the other treatments were considered as the binding partners of the ligand used. When the cells were treated with TriCEPS coupled transferrin, the transferrin receptor protein (TFR1) was enriched (left side of the volcano plot), whereas in the ligand of interest treated samples the MUC5B was enriched. Thus, MUC5B was identified as receptor for PRP-1 (Fig. 1B). The data of the experiment was presented in biological triplicates. The P-value obtained for every protein was plotted against the log2 of the magnitude of the fold enrichment. The space for positive control receptors and high-confidence receptor candidates was designated and visualized based on (fold-change >4) significant enrichment (adjusted P<0.01). True positive receptor candidates that contain only few tryptic peptides can be enriched substantially but will rarely get adjusted P<0.01. For the final selection of receptor candidates for follow-up investigations, all proteins in the receptor space should be viewed based on the following

Table I. PRP-1 effect on GPCR receptors (agonist mode).

GPCR ID	Assay mode	Conc (µM)	Mean RLU	% Activity
ADCYAP1R1	Agonist	6	271200	1
ADORA3	Agonist	6	213700	1
ADRA1B	Agonist	6	372900	1
ADRA2A	Agonist	6	312500	0
ADRA2B	Agonist	6	315400	4
ADRA2C	Agonist	6	296300	0
ADRB1	Agonist	6	184300	1
ADRB2	Agonist	6	18800	3
AGTR1	Agonist	6	424900	2
AGTRL1	Agonist	6	429300	1
AVPR1A	Agonist	6	23600	0
AVPR1B	Agonist	6	35200	0
AVPR2	Agonist	6	822800	0
BDKRB1	Agonist	6	30100	1
BDKRB2	Agonist	6	663600	0
BRS3	Agonist	6	209300	0
C3AR1	Agonist	6	55900	0
C5AR1	Agonist	6	119400	0
C5L2	Agonist	6	164800	0
CALCR	Agonist	6	42500	1
CALCRL-RAMP1	Agonist	6	92800	0
CALCRL-RAMP2	Agonist	6	219200	1
CALCRL-RAMP3	Agonist	6	425200	0
CALCR-RAMP2	Agonist	6	139500	2
CALCR-RAMP3	Agonist	6	28600	7
CCKAR	Agonist	6	44600	0
CCKBR	Agonist	6	894800	0
CCR10	Agonist	6	93400	0
CCR1	Agonist	6	540700	7
CCR2	Agonist	6	67000	0
CCR3	Agonist	6	272100	2
CCR4	Agonist	6	180300	0
CCR5	Agonist	6	89800	0
CCR6	Agonist	6	141000	0
CCR7	Agonist	6	766200	1
CCR8	Agonist	6	35900	0
CCR9	Agonist	6	119300	1
CHRM1	Agonist	6	1181100	1
CHRM2	Agonist	6	54600	1
CHRM3	Agonist	6	166300	2
CHRM4	Agonist	6	787900	16
CHRM5	Agonist	6	2995100	5
CMKLR1	Agonist	6	81900	0
CNR1	Agonist	6	80000	0
CNR2	Agonist	6	315400	-2
CRHR1	Agonist	6	361400	1
CRHR2	Agonist	6	161100	0
CRTH2	Agonist	6	172600	0
CX3CR1	Agonist	6	342700	1
CXCR1	Agonist	6	219900	0
CXCR2	Agonist	6	165200	1

Table I. Continued.

GPCR ID	Assay mode	Conc (µM)	Mean RLU	% Activity
CXCR3	Agonist	6	387900	1
CXCR4	Agonist	6	72500	2
CXCR5	Agonist	6	230900	1
CXCR6	Agonist	6	27700	2
CXCR7	Agonist	6	194500	0
DRD1	Agonist	6	73000	0
DRD2L	Agonist	6	83500	0
DRD2S	Agonist	6	247200	0
DRD3	Agonist	6	414700	2
DRD4	Agonist	6	22800	3
DRD5	Agonist	6	21000	1
EBI2	Agonist	6	150100	0
EDG1	Agonist	6	165500	0
EDG3	Agonist	6	877900	0
EDG4	Agonist	6	234300	4
EDG5	Agonist	6	174300	1
EDG6	Agonist	6	574100	-2
EDG7	Agonist	6	154400	0
EDNRA	Agonist	6	38500	0
EDNRB	Agonist	6	68900	0
F2R	Agonist	6	470700	-2
F2RL1	Agonist	6	566200	0
F2RL3	Agonist	6	909900	-1
FFAR1	Agonist	6	560800	3
FPR1	Agonist	6	1133900	4
FPRL1	Agonist	6	63900	0
FSHR	Agonist	6	197900	-2
GALR1	Agonist	6	263400	1
GALR2	Agonist	6	307700	1
GCGR	Agonist	6	295600	0
GHSR	Agonist	6	524600	2
GIPR	Agonist	6	17500	-1
GLP1R	Agonist	6	123500	0
GLP2R	Agonist	6	101400	1
GPR1	Agonist	6	58400	0
GPR103	Agonist	6	45100	2
GPR109A	Agonist	6	458200	4
GPR109B	Agonist	6	410400	1
GPR119	Agonist	6	289300	3
GPR120	Agonist	6	27800	1
GPR35	Agonist	6	287100	1
GPR92	Agonist	6	257600	1
GRPR	Agonist	6	39000	0
HCRTR1	Agonist	6	45600	0
HCRTR2	Agonist	6	69900	0
HRH1	Agonist	6	345600	1
HRH2	Agonist	6	91300	1
HRH3	Agonist	6	47100	2
HRH4	Agonist	6	910300	4
HTR1A	Agonist	6	879000	0
HTR1B	Agonist	6	1214900	-4

Table I. Continued.

GPCR ID	Assay mode	Conc (μM)	Mean RLU	% Activity
HTR1E	Agonist	6	2963300	3
HTR1F	Agonist	6	345900	2
HTR2A	Agonist	6	455100	1
HTR2C	Agonist	6	921600	1
HTR5A	Agonist	6	990000	0
KISS1R	Agonist	6	45800	1
LHCGR	Agonist	6	24700	0
LTB4R	Agonist	6	187300	1
MC1R	Agonist	6	17000	-2
MC3R	Agonist	6	25100	3
MC4R	Agonist	6	25900	-1
MC5R	Agonist	6	54900	2
MCHR1	Agonist	6	140300	1
MCHR2	Agonist	6	62800	1
MLNR	Agonist	6	227800	1
MRGPRX1	Agonist	6	869600	1
MRGPRX2	Agonist	6	355800	0
MTNR1A	Agonist	6	79100	2
NMBR	Agonist	6	62800	0
NMU1R	Agonist	6	98100	1
NPBWR1	Agonist	6	69600	3
NPBWR2	Agonist	6	169400	1
NPFFR1	Agonist	6	131100	3
NPSR1B	Agonist	6	89900	2
NPY1R	Agonist	6	106100	0
NPY2R	Agonist	6	362000	0
NTSR1	Agonist	6	313400	0
OPRD1	Agonist	6	91200	0
OPRK1	Agonist	6	36400	0
OPRL1	Agonist	6	229600	0
OPRM1	Agonist	6	137000	1
OXER1	Agonist	6	86900	-2
OXTR	Agonist	6	25800	0
P2RY1	Agonist	6	123800	-1
P2RY11	Agonist	6	68900	1
P2RY12	Agonist	6	250500	1
P2RY2	Agonist	6	384500	2
P2RY4	Agonist	6	397000	-1
P2RY6	Agonist	6	324200	0
PPYR1	Agonist	6	34900	0
PRLHR	Agonist	6	35900	4
PROKR1	Agonist	6	49600	2
PROKR2	Agonist	6	15700	0
PTAFR	Agonist	6	480900	1
PTGER2	Agonist	6	30800	4
PTGER3	Agonist	6	246700	1
PTGER4	Agonist	6	95700	1
PTGFR	Agonist	6	16400	0
PTGIR	Agonist	6	135100	1
PTHR1	Agonist	6	129100	1
PTHR2	Agonist	6	123100	0

Table I. Continued.

GPCR ID	Assay mode	Conc (μM)	Mean RLU	% Activity
RXFP3	Agonist	6	149000	6
SCTR	Agonist	6	502600	1
SSTR1	Agonist	6	15000	-3
SSTR2	Agonist	6	11800	0
SSTR3	Agonist	6	82000	1
SSTR5	Agonist	6	176900	1
TACR1	Agonist	6	702100	1
TACR2	Agonist	6	415100	1
TACR3	Agonist	6	145800	0
TBXA2R	Agonist	6	203300	1
TRHR	Agonist	6	27600	1
TSHR(L)	Agonist	6	9600	4
UTR2	Agonist	6	31200	3
VIPR1	Agonist	6	399800	0
VIPR2	Agonist	6	342300	1

parameters: proteins that were increased >4 times (log2=2 on the x-axis) with adjusted P<0.01 [-log (0.01)=2] were considered to be in the receptor space (white). The protter figure (Fig. 1C) usually displays peptides belonging to the ligand's receptor as being enriched (shown in highlighted stripes) compared with the control sample (no ligand). Protter is an interactive tool for protein data analysis (47). The experimental results with MUC5B ELISA confirmed the binding, PRP-1 at 1 μg/ml detected MUC5B presence at 440 ng/ml in the cell lysates of human JJ012 chondrosarcoma cells (Fig. 1D). Toll like receptors TLR1/2 and TLR6 were identified by western blot as binding interaction partners with PRP-1 in human chondrosarcoma JJ012 cell line lysates. Polyacrylamide gel electrophoresis, immunoblot results indicated that PRP-1 caused strong upregulation of TLR1 and TLR2 in comparison to untreated control. TLR3 expression was present but weak and data is not shown. TLR4 and TLR5 were expressed, but PRP-1 did not have any effect (Fig. 2). TLR6 protein expression was also increased in dose-dependent manner in PRP-1 treated samples. TLR7 was not expressed at all in the cell line, whereas TLR8, 9 and 10 were expressed but there was no indication of PRP-1 effect (Fig. 2). Thus, TLR1/2 and TLR6 were identified as interacting binding partners for PRP-1. Fig. 2 depicts the PRP-1 action on the protein expression of the adaptors TICAM1 (TRIF) and TICAM2 (TRAM). PRP-1 upregulated in dose-dependent manner the adaptor TICAM2 but not TICAM1. Toll like receptors TLR1/2 and TLR6 and MUC5B were detected with PRP-1 in the nucleus of human chondrosarcoma cells by immunocytochemistry. Since the experiments with immunoblot and TriCEPS indicated that cell surface receptors TLR1/2, TLR6 and gel forming mucin MUC5B were the binding partners for PRP-1, the immunocytochemistry experiments followed next; not only to prove PRP-1 endogenous presence in chondrosarcoma, but also its cellular colocalization with the binding partners. The images are displayed in Fig. 3. PRP-1 antibody, isolated from rabbit
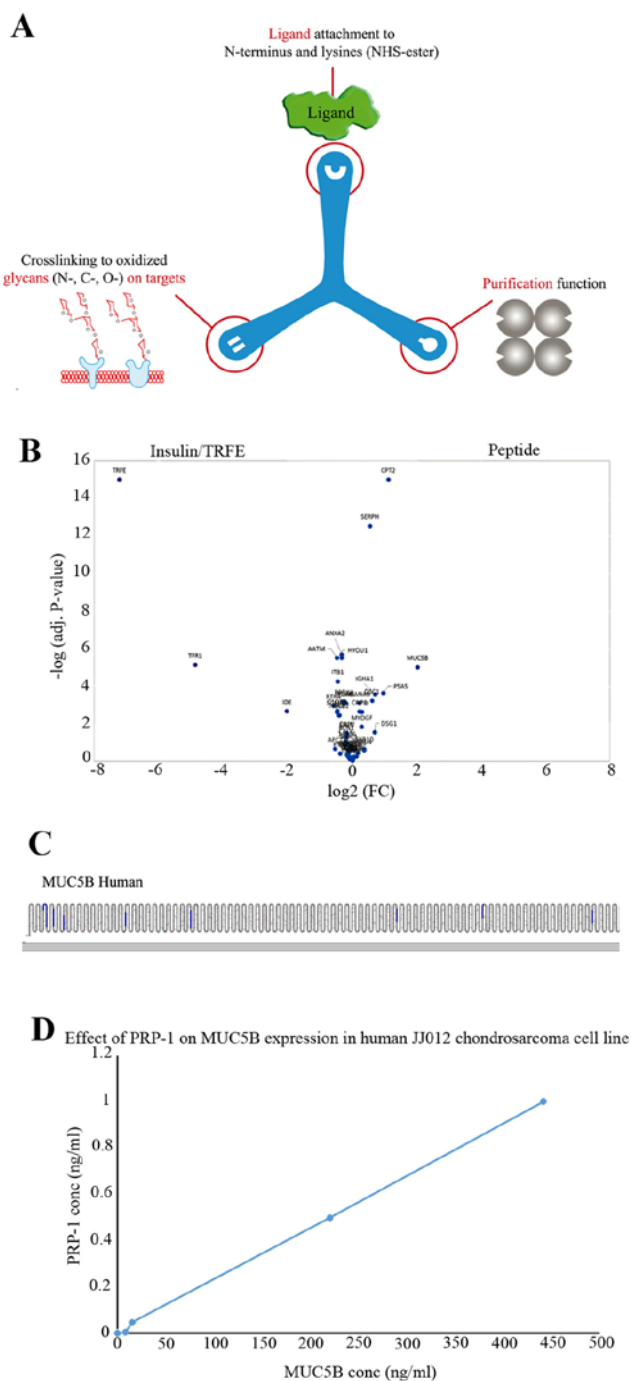
A

B

C

MUC5B Human

D

Figure 1. Identification of PRP-1 receptor binding protein MUC5B by Ligand-receptor capture technology (LRC) and human MUC5B ELISA in JJ012 chondrosarcoma cell line. (A) Ligand-receptor capture technology (LRC). Three orthogonal functionalities in TRICEPS-one arm binding an amino group containing ligands, a second arm that captures ligand with glycosylated receptors and the third arm has a biotin tag for purifying receptor peptides to be detected by quantitative mass spectrometry (MS). (B) Volcano plot. LRC-TriCEPS volcano plot compares the proteins that are enriched in the control samples (left side, x-axes Value -2 till -8) include enriched TRF1 = Transferrin receptor (true positive) and borderline IDE, insulin-degrading enzyme compared to the ligand of interest, (PRP-1) samples (on the right) in human chondrosarcoma cells. On the right side of the volcano plot (x-axes Value +2 till +8) the target MUC5B of ligand of interest (PRP-1) is depicted. On the x-axis log2 of the fold change of the quantified protein comparing the samples of the ligand of interest with the control. On the y-axis the -log (adj. P-value) as the experiment was performed in triplicates. (C) Protter. In the protter picture the tryptic peptides (highlighted) that are identified by LC-MS/MS measurement for MUC5B. (D) Human MUC5B ELISA in the cell lysates of human JJ012 chondrosarcoma cells. PRP-1 at 1 μg/ml detected MUC5B presence at 440 ng/ml (D).

Table II. PRP-1 effect on GPCR receptors (antagonist mode).

GPCR ID	Assay mode	Conc (μM)	Mean RLU	% Inhibition
ADCYAP1R1	Antagonist	6	1676100	-6
ADORA3	Antagonist	6	891300	-3
ADRA1B	Antagonist	6	2076200	0
ADRA2A	Antagonist	6	1075700	0
ADRA2B	Antagonist	6	856100	2
ADRA2C	Antagonist	6	1511200	-4
ADRB1	Antagonist	6	674600	-5
ADRB2	Antagonist	6	179900	-3
AGTR1	Antagonist	6	2568500	0
AGTRL1	Antagonist	6	2263600	0
AVPR1A	Antagonist	6	789300	-1
AVPR1B	Antagonist	6	258900	-2
AVPR2	Antagonist	6	3487000	0
BDKRB1	Antagonist	6	225900	-8
BDKRB2	Antagonist	6	4293900	5
BRS3	Antagonist	6	1248800	4
C3AR1	Antagonist	6	1933800	-2
C5AR1	Antagonist	6	2029300	3
C5L2	Antagonist	6	547000	-5
CALCR	Antagonist	6	358200	1
CALCRL-RAMP1	Antagonist	6	1395000	4
CALCRL-RAMP2	Antagonist	6	892100	-1
CALCRL-RAMP3	Antagonist	6	2293600	1
CALCR-RAMP2	Antagonist	6	698200	0
CALCR-RAMP3	Antagonist	6	59000	-8
CCKAR	Antagonist	6	1490300	-3
CCKBR	Antagonist	6	3697600	-3
CCR10	Antagonist	6	1295800	-3
CCR1	Antagonist	6	1214200	-3
CCR2	Antagonist	6	1380800	-3
CCR3	Antagonist	6	1136200	-3
CCR4	Antagonist	6	2075100	2
CCR5	Antagonist	6	2359300	-2
CCR6	Antagonist	6	1487700	2
CCR7	Antagonist	6	3413600	-2
CCR8	Antagonist	6	1376000	-4
CCR9	Antagonist	6	1538300	-6
CHRM1	Antagonist	6	2892100	-12
CHRM2	Antagonist	6	540500	-6
CHRM3	Antagonist	6	1187400	-6
CHRM4	Antagonist	6	1390200	-18
CHRM5	Antagonist	6	4585200	-4
CMKLR1	Antagonist	6	3258400	-2
CNR1	Antagonist	6	377300	2
CNR2	Antagonist	6	580500	5
CRHR1	Antagonist	6	4103800	1
CRHR2	Antagonist	6	2968600	-2
CRTH2	Antagonist	6	1149200	-8
CX3CR1	Antagonist	6	3207000	2
CXCR1	Antagonist	6	3818300	-1
CXCR2	Antagonist	6	565700	-3

Table II. Continued.

GPCR ID	Assay mode	Conc (μM)	Mean RLU	% Inhibition
CXCR3	Antagonist	6	1392600	-1
CXCR4	Antagonist	6	139700	2
CXCR5	Antagonist	6	1098600	-8
CXCR6	Antagonist	6	101400	-6
CXCR7	Antagonist	6	2856200	-2
DRD1	Antagonist	6	696300	-5
DRD2L	Antagonist	6	393800	2
DRD2S	Antagonist	6	1242000	6
DRD3	Antagonist	6	1263000	-15
DRD4	Antagonist	6	65500	-2
DRD5	Antagonist	6	149600	-8
EBI2	Antagonist	6	2425000	-1
EDG1	Antagonist	6	936700	0
EDG3	Antagonist	6	4548500	1
EDG4	Antagonist	6	657500	5
EDG5	Antagonist	6	2180100	-8
EDG6	Antagonist	6	1169200	4
EDG7	Antagonist	6	1432500	-3
EDNRA	Antagonist	6	953300	0
EDNRB	Antagonist	6	1248000	-1
F2R	Antagonist	6	1612200	-16
F2RL1	Antagonist	6	3638100	3
F2RL3	Antagonist	6	3027600	-1
FFAR1	Antagonist	6	1070500	0
FPR1	Antagonist	6	3077200	-4
FPRL1	Antagonist	6	2991600	-2
FSHR	Antagonist	6	621700	-2
GALR1	Antagonist	6	1759100	-4
GALR2	Antagonist	6	1686800	-11
GCGR	Antagonist	6	3115100	-4
GHSR	Antagonist	6	2068100	-6
GIPR	Antagonist	6	79600	-24
GLP1R	Antagonist	6	1983100	-9
GLP2R	Antagonist	6	727800	-11
GPR1	Antagonist	6	1076400	-5
GPR103	Antagonist	6	103800	6
GPR109A	Antagonist	6	1141200	-4
GPR109B	Antagonist	6	2871700	-6
GPR119	Antagonist	6	521500	-1
GPR120	Antagonist	6	130400	-6
GPR35	Antagonist	6	910400	-6
GPR92	Antagonist	6	854500	12
GRPR	Antagonist	6	1570000	-7
HCRTR1	Antagonist	6	3242300	0
HCRTR2	Antagonist	6	2611400	-1
HRH1	Antagonist	6	1912200	0
HRH2	Antagonist	6	347800	1
HRH3	Antagonist	6	180200	-6
HRH4	Antagonist	6	2264500	-9
HTR1A	Antagonist	6	2576600	-5
HTR1B	Antagonist	6	2334400	4

Table II. Continued.

GPCR ID	Assay mode	Conc (μM)	Mean RLU	% Inhibition
HTR1E	Antagonist	6	5487000	5
HTR1F	Antagonist	6	982500	2
HTR2A	Antagonist	6	3103200	-5
HTR2C	Antagonist	6	4188400	-3
HTR5A	Antagonist	6	4536500	0
KISS1R	Antagonist	6	270900	3
LHCGR	Antagonist	6	144000	-15
LTB4R	Antagonist	6	1844800	0
MC1R	Antagonist	6	69300	-2
MC3R	Antagonist	6	153200	-6
MC4R	Antagonist	6	128200	-6
MC5R	Antagonist	6	179900	-5
MCHR1	Antagonist	6	1023000	-4
MCHR2	Antagonist	6	530900	-3
MLNR	Antagonist	6	2032800	-7
MRGPRX1	Antagonist	6	3890200	-2
MRGPRX2	Antagonist	6	1945500	-8
MTNR1A	Antagonist	6	241200	-9
NMBR	Antagonist	6	720100	-5
NMU1R	Antagonist	6	985900	-3
NPBWR1	Antagonist	6	188200	0
NPBWR2	Antagonist	6	1070300	-3
NPFFR1	Antagonist	6	290800	-3
NPSR1B	Antagonist	6	699900	0
NPY1R	Antagonist	6	973600	4
NPY2R	Antagonist	6	3477300	-2
NTSR1	Antagonist	6	2192400	-1
OPRD1	Antagonist	6	795800	-2
OPRK1	Antagonist	6	215800	-12
OPRL1	Antagonist	6	1062000	-7
OPRM1	Antagonist	6	2828200	-2
OXER1	Antagonist	6	246400	-16
OXTR	Antagonist	6	540000	1
P2RY1	Antagonist	6	530600	1
P2RY11	Antagonist	6	484300	-12
P2RY12	Antagonist	6	699600	8
P2RY2	Antagonist	6	1093000	-4
P2RY4	Antagonist	6	1323200	0
P2RY6	Antagonist	6	1825600	3
PPYR1	Antagonist	6	276600	-4
PRLHR	Antagonist	6	122100	-3
PROKR1	Antagonist	6	499800	-2
PROKR2	Antagonist	6	111500	8
PTAFR	Antagonist	6	3532600	-8
PTGER2	Antagonist	6	72100	-11
PTGER3	Antagonist	6	967100	-2
PTGER4	Antagonist	6	852400	4
PTGFR	Antagonist	6	453000	1
PTGIR	Antagonist	6	380600	-2
PTHR1	Antagonist	6	2941200	-2
PTHR2	Antagonist	6	2882300	-1

Table II. Continued.

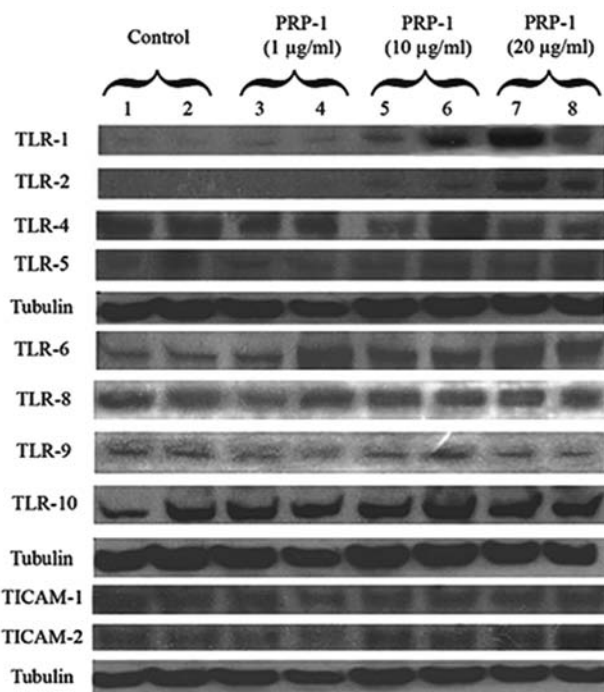| GPCR ID	Assay mode	Conc (μM)	Mean RLU	% Inhibition
RXFP3	Antagonist	6	330200	-3
SCTR	Antagonist	6	3424900	-2
SSTR1	Antagonist	6	38300	-14
SSTR2	Antagonist	6	797000	-11
SSTR3	Antagonist	6	771000	-5
SSTR5	Antagonist	6	1327400	-11
TACR1	Antagonist	6	4862800	-2
TACR2	Antagonist	6	2331100	0
TACR3	Antagonist	6	2745900	-1
TBXA2R	Antagonist	6	1032900	-10
TRHR	Antagonist	6	301600	-5
TSHR(L)	Antagonist	6	83000	-4
UTR2	Antagonist	6	156000	-7
VIPR1	Antagonist	6	3344300	-9
VIPR2	Antagonist	6	3604300	-3

Figure 2. PRP-1 effect on TLR receptors and adaptor proteins in human chondrosarcoma JJ012 cell line. PRP-1 upregulated protein expression of TLR1 and TLR2 in dose-dependent manner in human JJ012 chondrosarcoma cell lysates. TLR3 expression was very weak and the data is not shown. TLR4, TLR5 proteins were expressed but PRP-1 did not have any effect. Tubulin was used as loading control. The bands were detected for TLR1, TLR2, TLR4 and TLR5 and tubulin at 120, 119, 130, 90 and 50 kDa, correspondingly. PRP-1 upregulated protein expression of TLR6 in dose-dependent manner in human JJ012 chondrosarcoma cell lysates. TLR7 was not expressed in this cell line at all. TLR8, 9 and 10 were expressed but no effect of PRP-1 was observed. Tubulin was used as housekeeping control. The bands were detected for TLR6, TLR8, TLR9, TLR10 and tubulin at 100, 86, 100, 120 and 50 kDa, correspondingly. PRP-1 upregulated TICAM2 (TRAM) adaptor protein in dose-response manner but did not have any effect on TICAM1 (TRIF) adaptor protein in human JJ012 chondrosarcoma cell line. Tubulin was used as loading control. The bands were detected for TICAM1, TICAM2 and tubulin.

Table III. PRP-1 effect on orphan receptors (agonist mode).

GPCR ID	Assay mode	Conc (μM)	Mean RLU	% Inhibition
ADCYAP1R1	Antagonist	6	1676100	-6
ADORA3	Antagonist	6	891300	-3
ADRA1B	Antagonist	6	2076200	0
ADRA2A	Antagonist	6	1075700	0
ADRA2B	Antagonist	6	856100	2
ADRA2C	Antagonist	6	1511200	-4
ADRB1	Antagonist	6	674600	-5
ADRB2	Antagonist	6	179900	-3
AGTR1	Antagonist	6	2568500	0
AGTRL1	Antagonist	6	2263600	0
AVPR1A	Antagonist	6	789300	-1
AVPR1B	Antagonist	6	258900	-2
AVPR2	Antagonist	6	3487000	0
BDKRB1	Antagonist	6	225900	-8
BDKRB2	Antagonist	6	4293900	5
BRS3	Antagonist	6	1248800	4
C3AR1	Antagonist	6	1933800	-2
C5AR1	Antagonist	6	2029300	3
C5L2	Antagonist	6	547000	-5
CALCR	Antagonist	6	358200	1
CALCRL-RAMP1	Antagonist	6	1395000	4
CALCRL-RAMP2	Antagonist	6	892100	-1
CALCRL-RAMP3	Antagonist	6	2293600	1
CALCR-RAMP2	Antagonist	6	698200	0
CALCR-RAMP3	Antagonist	6	59000	-8
CCKAR	Antagonist	6	1490300	-3
CCKBR	Antagonist	6	3697600	-3
CCR10	Antagonist	6	1295800	-3
CCR1	Antagonist	6	1214200	-3
CCR2	Antagonist	6	1380800	-3
CCR3	Antagonist	6	1136200	-3
CCR4	Antagonist	6	2075100	2
CCR5	Antagonist	6	2359300	-2
CCR6	Antagonist	6	1487700	2
CCR7	Antagonist	6	3413600	-2
CCR8	Antagonist	6	1376000	-4
CCR9	Antagonist	6	1538300	-6
CHRM1	Antagonist	6	2892100	-12
CHRM2	Antagonist	6	540500	-6
CHRM3	Antagonist	6	1187400	-6
CHRM4	Antagonist	6	1390200	-18
CHRM5	Antagonist	6	4585200	-4
CMKLR1	Antagonist	6	3258400	-2
CNR1	Antagonist	6	377300	2
CNR2	Antagonist	6	580500	5
CRHR1	Antagonist	6	4103800	1
CRHR2	Antagonist	6	2968600	-2
CRTH2	Antagonist	6	1149200	-8
CX3CR1	Antagonist	6	3207000	2
CXCR1	Antagonist	6	3818300	-1
CXCR2	Antagonist	6	565700	-3

Table III. Continued.

GPCR ID	Assay mode	Conc (μM)	Mean RLU	% Inhibition
CXCR3	Antagonist	6	1392600	-1
CXCR4	Antagonist	6	139700	2
CXCR5	Antagonist	6	1098600	-8
CXCR6	Antagonist	6	101400	-6
CXCR7	Antagonist	6	2856200	-2
DRD1	Antagonist	6	696300	-5
DRD2L	Antagonist	6	393800	2
DRD2S	Antagonist	6	1242000	6
DRD3	Antagonist	6	1263000	-15
DRD4	Antagonist	6	65500	-2
DRD5	Antagonist	6	149600	-8
EBI2	Antagonist	6	2425000	-1
EDG1	Antagonist	6	936700	0
EDG3	Antagonist	6	4548500	1
EDG4	Antagonist	6	657500	5
EDG5	Antagonist	6	2180100	-8
EDG6	Antagonist	6	1169200	4
EDG7	Antagonist	6	1432500	-3
EDNRA	Antagonist	6	953300	0
EDNRB	Antagonist	6	1248000	-1
F2R	Antagonist	6	1612200	-16
F2RL1	Antagonist	6	3638100	3
F2RL3	Antagonist	6	3027600	-1
FFAR1	Antagonist	6	1070500	0
FPR1	Antagonist	6	3077200	-4
FPRL1	Antagonist	6	2991600	-2
FSHR	Antagonist	6	621700	-2
GALR1	Antagonist	6	1759100	-4
GALR2	Antagonist	6	1686800	-11
GCGR	Antagonist	6	3115100	-4
GHSR	Antagonist	6	2068100	-6
GIPR	Antagonist	6	79600	-24
GLP1R	Antagonist	6	1983100	-9
GLP2R	Antagonist	6	727800	-11
GPR1	Antagonist	6	1076400	-5
GPR103	Antagonist	6	103800	6
GPR109A	Antagonist	6	1141200	-4
GPR109B	Antagonist	6	2871700	-6
GPR119	Antagonist	6	521500	-1
GPR120	Antagonist	6	130400	-6
GPR35	Antagonist	6	910400	-6
GPR92	Antagonist	6	854500	12
GRPR	Antagonist	6	1570000	-7
HCRTR1	Antagonist	6	3242300	0
HCRTR2	Antagonist	6	2611400	-1
HRH1	Antagonist	6	1912200	0
HRH2	Antagonist	6	347800	1
HRH3	Antagonist	6	180200	-6
HRH4	Antagonist	6	2264500	-9
HTR1A	Antagonist	6	2576600	-5
HTR1B	Antagonist	6	2334400	4

Table III. Continued.

GPCR ID	Assay mode	Conc (μM)	Mean RLU	% Inhibition
HTR1E	Antagonist	6	5487000	5
HTR1F	Antagonist	6	982500	2
HTR2A	Antagonist	6	3103200	-5
HTR2C	Antagonist	6	4188400	-3
HTR5A	Antagonist	6	4536500	0
KISS1R	Antagonist	6	270900	3
LHCGR	Antagonist	6	144000	-15
LTB4R	Antagonist	6	1844800	0
MC1R	Antagonist	6	69300	-2
MC3R	Antagonist	6	153200	-6
MC4R	Antagonist	6	128200	-6
MC5R	Antagonist	6	179900	-5
MCHR1	Antagonist	6	1023000	-4
MCHR2	Antagonist	6	530900	-3
MLNR	Antagonist	6	2032800	-7
MRGPRX1	Antagonist	6	3890200	-2
MRGPRX2	Antagonist	6	1945500	-8
MTNR1A	Antagonist	6	241200	-9
NMBR	Antagonist	6	720100	-5
NMU1R	Antagonist	6	985900	-3
NPBWR1	Antagonist	6	188200	0
NPBWR2	Antagonist	6	1070300	-3
NPFFR1	Antagonist	6	290800	-3
NPSR1B	Antagonist	6	699900	0
NPY1R	Antagonist	6	973600	4
NPY2R	Antagonist	6	3477300	-2
NTSR1	Antagonist	6	2192400	-1
OPRD1	Antagonist	6	795800	-2
OPRK1	Antagonist	6	215800	-12
OPRL1	Antagonist	6	1062000	-7
OPRM1	Antagonist	6	2828200	-2
OXER1	Antagonist	6	246400	-16
OXTR	Antagonist	6	540000	1
P2RY1	Antagonist	6	530600	1
P2RY11	Antagonist	6	484300	-12
P2RY12	Antagonist	6	699600	8
P2RY2	Antagonist	6	1093000	-4
P2RY4	Antagonist	6	1323200	0
P2RY6	Antagonist	6	1825600	3
PPYR1	Antagonist	6	276600	-4
PRLHR	Antagonist	6	122100	-3
PROKR1	Antagonist	6	499800	-2
PROKR2	Antagonist	6	111500	8
PTAFR	Antagonist	6	3532600	-8
PTGER2	Antagonist	6	72100	-11
PTGER3	Antagonist	6	967100	-2
PTGER4	Antagonist	6	852400	4
PTGFR	Antagonist	6	453000	1
PTGIR	Antagonist	6	380600	-2
PTHR1	Antagonist	6	2941200	-2
PTHR2	Antagonist	6	2882300	-1

Table III. Continued.

GPCR ID	Assay mode	Conc (μM)	Mean RLU	% Inhibition
RXFP3	Antagonist	6	330200	-3
SCTR	Antagonist	6	3424900	-2
SSTR1	Antagonist	6	38300	-14
SSTR2	Antagonist	6	797000	-11
SSTR3	Antagonist	6	771000	-5
SSTR5	Antagonist	6	1327400	-11
TACR1	Antagonist	6	4862800	-2
TACR2	Antagonist	6	2331100	0
TACR3	Antagonist	6	2745900	-1
TBXA2R	Antagonist	6	1032900	-10
TRHR	Antagonist	6	301600	-5
TSHR(L)	Antagonist	6	83000	-4
UTR2	Antagonist	6	156000	-7
VIPR1	Antagonist	6	3344300	-9
VIPR2	Antagonist	6	3604300	-3
ADCYAP1R1	Agonist	6	271200	1
ADORA3	Agonist	6	213700	1
ADRA1B	Agonist	6	372900	1
ADRA2A	Agonist	6	312500	0
ADRA2B	Agonist	6	315400	4
ADRA2C	Agonist	6	296300	0
ADRB1	Agonist	6	184300	1
ADRB2	Agonist	6	18800	3
AGTR1	Agonist	6	424900	2
AGTRL1	Agonist	6	429300	1
AVPR1A	Agonist	6	23600	0
AVPR1B	Agonist	6	35200	0
AVPR2	Agonist	6	822800	0
BDKRB1	Agonist	6	30100	1
BDKRB2	Agonist	6	663600	0
BRS3	Agonist	6	209300	0
C3AR1	Agonist	6	55900	0
C5AR1	Agonist	6	119400	0
C5L2	Agonist	6	164800	0
CALCR	Agonist	6	42500	1
CALCRL-RAMP1	Agonist	6	92800	0
CALCRL-RAMP2	Agonist	6	219200	1
CALCRL-RAMP3	Agonist	6	425200	0
CALCR-RAMP2	Agonist	6	139500	2
CALCR-RAMP3	Agonist	6	28600	7
CCKAR	Agonist	6	44600	0
CCKBR	Agonist	6	894800	0
CCR10	Agonist	6	93400	0
CCR1	Agonist	6	540700	7
CCR2	Agonist	6	67000	0
CCR3	Agonist	6	272100	2
CCR4	Agonist	6	180300	0
CCR5	Agonist	6	89800	0
CCR6	Agonist	6	141000	0
CCR7	Agonist	6	766200	1

Table III. Continued.

GPCR ID	Assay mode	Conc (μM)	Mean RLU	% Inhibition
CCR8	Agonist	6	35900	0
CCR9	Agonist	6	119300	1
CHRM1	Agonist	6	1181100	1
CHRM2	Agonist	6	54600	1
CHRM3	Agonist	6	166300	2
CHRM4	Agonist	6	787900	16
CHRM5	Agonist	6	2995100	5
CMKLR1	Agonist	6	81900	0
CNR1	Agonist	6	80000	0
CNR2	Agonist	6	315400	-2
CRHR1	Agonist	6	361400	1
CRHR2	Agonist	6	161100	0
CRTH2	Agonist	6	172600	0
CX3CR1	Agonist	6	342700	1
CXCR1	Agonist	6	219900	0
CXCR2	Agonist	6	165200	1
CXCR3	Agonist	6	387900	1
CXCR4	Agonist	6	72500	2
CXCR5	Agonist	6	230900	1
CXCR6	Agonist	6	27700	2
CXCR7	Agonist	6	194500	0
DRD1	Agonist	6	73000	0
DRD2L	Agonist	6	83500	0
DRD2S	Agonist	6	247200	0
DRD3	Agonist	6	414700	2
DRD4	Agonist	6	22800	3
DRD5	Agonist	6	21000	1
EBI2	Agonist	6	150100	0
EDG1	Agonist	6	165500	0
EDG3	Agonist	6	877900	0
EDG4	Agonist	6	234300	4
EDG5	Agonist	6	174300	1
EDG6	Agonist	6	574100	-2
EDG7	Agonist	6	154400	0
EDNRA	Agonist	6	38500	0
EDNRB	Agonist	6	68900	0
F2R	Agonist	6	470700	-2
F2RL1	Agonist	6	566200	0
F2RL3	Agonist	6	909900	-1
FFAR1	Agonist	6	560800	3
FPR1	Agonist	6	1133900	4
FPRL1	Agonist	6	63900	0
FSHR	Agonist	6	197900	-2
GALR1	Agonist	6	263400	1
GALR2	Agonist	6	307700	1
GCGR	Agonist	6	295600	0
GHSR	Agonist	6	524600	2
GIPR	Agonist	6	17500	-1
GLP1R	Agonist	6	123500	0

Table IV. PRP-1 activity with nhrMAX panel.

Assay format	Assay target	Conc (μM)	Value 1	Value 2	Average value	SD	% Efficacy
Agonist	AR	6	3600	3200	3400	282.84	-0.3
Antagonist	AR	6	17200	17400	17300	141.42	4.3
Agonist	ERalpha	6	50400	50000	50200	282.84	0.6
Antagonist	ERalpha	6	293600	288200	290900	3818.4	-2.8
Antagonist	ERRalpha	6	65800	61200	63500	3252.7	-4.7
Inverse agonist	ERRalpha	6	134600	120000	127300	10324	-7.2
Agonist	FXR	6	4000	6200	5100	1555.6	0.9
Antagonist	FXR	6	95400	103400	99400	5656.9	-4.5
Agonist	GR	6	15200	16800	16000	1131.4	0.3
Antagonist	GR	6	999800	1086200	1043000	61094	-9.7
Agonist	LXRalpha	6	232800	216800	224800	11314	-0.6
Antagonist	LXRalpha	6	1660000	1807600	1733800	104370	-10.7
Agonist	LXRbeta	6	311400	330200	320800	13294	1.6
Antagonist	LXRbeta	6	1208200	1379200	1293700	120920	-4
Agonist	MR	6	16200	18000	17100	1272.8	0.3
Antagonist	MR	6	295400	303800	299600	5939.7	-0.7
Agonist	PPARalpha	6	14600	15000	14800	282.84	0.9
Antagonist	PPARalpha	6	108400	105000	106700	2404.2	-3.3
Agonist	PPARdelta	6	1077800	1247000	1162400	119640	0.9
Antagonist	PPARdelta	6	3209000	2884800	3046900	229240	2.2
Agonist	PPARgamma	6	4400	5800	5100	989.95	0.3
Antagonist	PPARgamma	6	29600	28400	29000	848.53	6.5
Agonist	PRalpha	6	25800	22800	24300	2121.3	-1.6
Antagonist	PRalpha	6	185400	190400	187900	3535.5	-3.1
Agonist	PRbeta	6	3200	2400	2800	565.69	1.4
Antagonist	PRbeta	6	28600	33600	31100	3535.5	-0.6
Agonist	RARalpha	6	29400	44800	37100	10889	-3.3
Antagonist	RARalpha	6	104000	106800	105400	1979.9	14
Agonist	RARbeta	6	263600	243600	253600	14142	-3.9
Antagonist	RARbeta	6	475000	572200	523600	68731	-0.5
Agonist	RXRalpha	6	226000	230000	228000	2828.4	-3.8
Antagonist	RXRalpha	6	851800	821400	836600	21496	0
Agonist	RXRgamma	6	367800	354200	361000	9616.7	-2.7
Antagonist	RXRgamma	6	1266600	1310200	1288400	30830	-1.2
Agonist	THRalpha	6	43400	34600	39000	6222.5	-0.2
Antagonist	THRalpha	6	383000	415800	399400	23193	-4.8
Agonist	THRbeta	6	732400	819600	776000	61660	9.3
Antagonist	THRbeta	6	1274000	1246600	1260300	19375	-5.2

SD, standard deviation.

serum and affinity chromatography purified was labeled with Zenon Alexa Fluor 488 IgG complex (green) and manifested its presence in the nucleus (labeled with DAPI in blue) of the chondrosarcoma cells (Fig. 3A). The green speckles and dots can be seen both inside and outside the nucleus. In the separate experiment without PRP-1 we have demonstrated that MUC5B is present in the nucleus of these cells as well (Fig. 3B). The plasma membrane is seen in red and MUC5B, which was labeled with DyLight 488 is green. The composite image (Fig. 3C) demonstrates nuclear localization of both MUC5B (left panel) and PRP-1 (right panel) in aqua green color on the background of blue nucleus. Fig. 3D illustrates the presence of TLR1 receptor, (labeled in yellow with H&L DyLight 550) in the nucleus and around it. Fig. 3E depicts colocalization experiment of TLR6 and PRP-1 and whereas it was problematic to show TLR1 and PRP-1 colocalization in the previous figure due to spectral overlaps, here TLR6 receptor nuclear and cytoplasmic localization is demonstrated
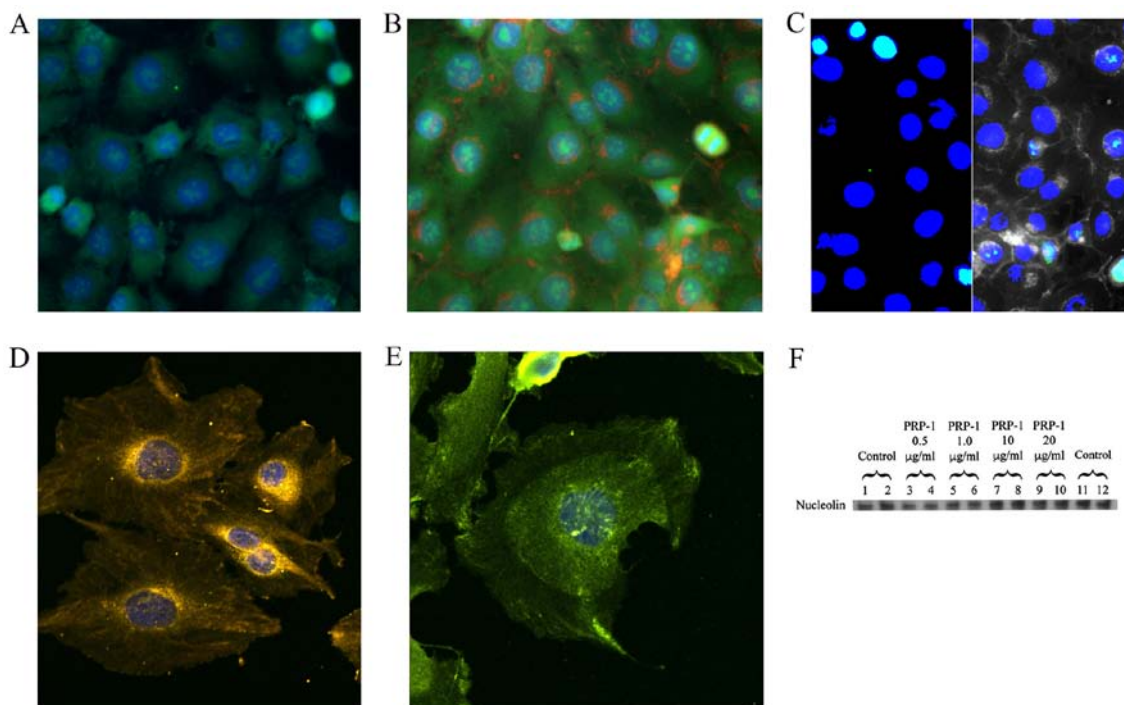
Figure 3. Immunocytochemistry results indicating nuclear localization of PRP-1 and nuclear colocalization with MUC5B, TLR1, TLR6 in human chondrosarcoma JJ012 cell line. (A) PRP-1 antibody localization in nucleus of human chondrosarcoma JJ012 cells. Dark blue color-DAPI was applied for nuclear staining. Zenon Alexa fluor rabbit 488IgG (green) was used for PRP-1 rabbit serum IgG antibody staining. (B) MUC5B receptor localization in the nucleus of human JJ012 chondrosarcoma cells. Alexa Fluor 594 wheat germ agglutinin (WGA) was used to label plasma membrane (red) at 1:200 dilution for 1 h. DAPI (dark blue) stained nucleus at 3 μM. Rabbit anti-MUC5B was adopted as primary, and green goat anti-rabbit IgG H&L (DyLight 488) was used as a secondary antibody. (C) Composite image of nuclear localization of MUC5B (left panel) and PRP-1 antibody (right panel) in human JJ012 chondrosarcoma cells. Dark blue color-DAPI was applied for nuclear staining. Zenon Alexa Fluor rabbit 488IgG (green) was used for PRP-1 rabbit serum IgG antibody detection. Rabbit anti-MUC5B was adopted as primary, and green goat anti-rabbit IgG H&L (DyLight 488) was used as a secondary antibody. (D) TLR1 receptor localization in the cytoplasm and the nucleus in human chondrosarcoma JJ012 cells. TLR1 rabbit antibody was used as a primary, whereas goat anti-rabbit H&L (DyLight 550) was applied as the secondary antibody (yellow color). (E) TLR6 receptor nuclear and cytoplasmic colocalization with PRP-1 is demonstrated, H&L DyLight 550 was used as a secondary antibody (yellow). PRP-1 was stained with Zenon Alexa Fluor 488 IgG (green). (F) Western blot of nucleolin protein expression in human chondrosarcoma cell line. PRP-1 did not have any effect on nucleolin expression, indicating the absence of PRP-1 location in nucleoli. The band corresponded to MW of 77 kDa.
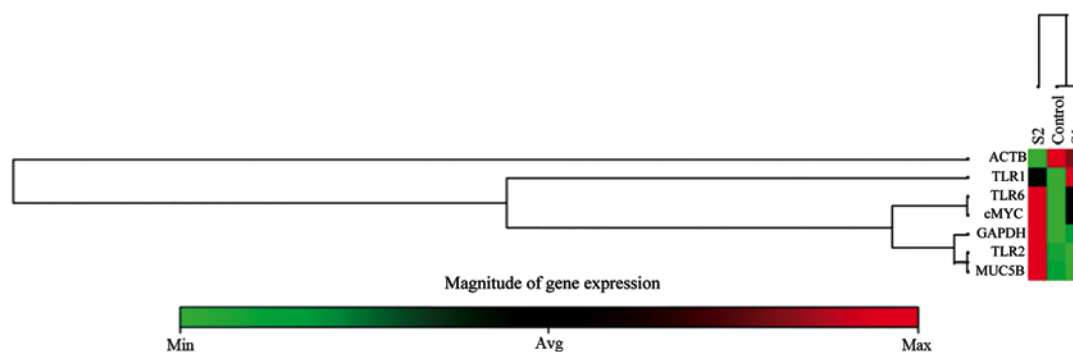
Figure 4. Heat map of gene expression (qRT PCR) upon PRP-1 treatment. The clustrogram performs non-supervised hierarchical clustering of the entire dataset to display a heat map with dendrograms indicating co-regulated genes across groups or individual samples; it represents the average of Ct values displayed across the genes of each sample. S2 stands for samples treated with 1 μg/ml of PRP-1 and S1 stands for 10 μg/ml of PRP-1. TLR2 and TLR6 were highly expressed in S2, while TLR1 was highly expressed in S1 and moderately in S2 group. c-Myc and MUC5B were highly expressed in S2. GAPDH and ACTB were housekeeping genes.

with PRP-1, which was stained with Zenon Alexa Fluor 488 IgG (green). H&L DyLight 550 was used as a secondary antibody (yellow) for TLR6. The immunoblot experiment with the nucleolin antibody, marker for nucleoli indicated that PRP-1 was not located in the nucleoli, as no changes in nucleolin protein expression was observed on PRP-1 treatment (Fig. 3F).

RT2 qPCR primer assays show the effect of PRP-1 on gene expression of TLR receptors and MUC5B. RT2 qPCR custom designed primer assays were performed by Qiagen to understand the effect of PRP-1 on gene expression of TLR receptors and MUC5B. Mature RNA was isolated using RNA extraction according to the manufacturer's instructions. RNA
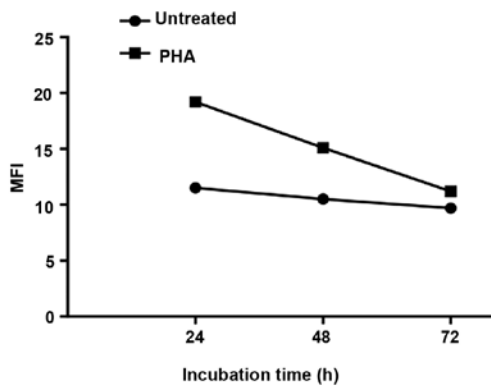
Figure 5. Immunostimulation triggers intracellular PRP-1 synthesis in normal resting and stimulated human peripheral blood lymphocytes. The dynamics of intracellular expression of PRP-1 in PHA-activated lymphocytes indicated that PRP-1 was induced at the early stages of cell activation. On y-axes (MFI)-median fluorescence intensity.

was subjected to spectrophotometrical quality control and then reverse transcribed to cDNA. RT2 SYBR-Green qPCR Master Mix was used with RT2 qPCR assays. In this study, 7 genes (TLR1, TLR2, TLR6, MUC5B, c-Myc and 2 housekeeping genes GAPDH and ACTB) were profiled on three samples with technical triplicates. c-Myc was included, as we wanted to confirm its drastic downregulation after PRP-1 treatment in luciferase assay (4) and western blot experiments, reported earlier (10). The heat map, clustergram of average Ct values across the gene of each sample, with the magnitude of gene expression scale below, is presented in Fig. 4. As evident from the figure, there is dose-dependent effect of PRP-1 on the expression of the above mentioned genes, except the control housekeeping genes. The TLR1 receptor was well expressed in the cells treated with 10 µg/ml, whereas no expression was detected at 1 µg/ml peptide treatment. TLR2, TLR6, MUC5B demonstrated high expression with 1 µg/ml treatment when compared to nontreated control. c-Myc expression went down drastically when treated with 10 µg/ml PRP-1. The data analysis web portal calculated fold change/regulation using ΔΔCt method, in which ΔCt is calculated between gene of interest (GOI) and an average of housekeeping genes (HKG) followed by ΔΔCt calculations (ΔCt (experiment) - ΔCt (control). Fold change is then calculated using the $2^{-\Delta\Delta Ct}$ formula. The system detected only statistically significant upregulation (P<0.0001) of TLR2 for the samples treated with 1 µg/ml PRP-1, with 5.26-fold upregulation when calculated with the ΔΔCt.

Discussion

Metastatic chondrosarcoma is fatal because of metastatic spread and absence of the effective therapies. Therefore, search for new approaches is of the utmost importance. PRP-1, inhibits chondrosarcoma cell growth by >80% (4,6) it halts cell cycle progression in G1/S transition (6). This mTORC1 inhibitor, cytostatic peptide is potent upregulator of tumor suppressors and inhibitor of oncoproteins and embryonic stem cell markers (7-9). We have demonstrated also that intracellular expression of PRP-1 is associated with the early stages of lymphocyte activation by phytohemagglutinin, (PHA) (Fig. 5).

However, the interacting partners or receptors for this important peptide has not been identified. Using triCEPS (ligand based receptor capture technology), we were able to identify MUC5B, one of the members of mucin family as the receptor for PRP-1. Notably, proline rich proteins in saliva, different from the neuropeptide PRP-1, were found in reported literature to interact with mucins (48). Immunoblot results of this study indicated that TLR1, TLR2 (which are usually dimerized) and TLR6 are binding interaction partners for PRP-1, as their expression increased in dose-response manner upon PRP-1 treatment. Indeed, the link between TLR1/2 and TLR6 was documented in the literature. TLR1 and TLR6 was shown to pair with TLR2 and that interaction was needed for pattern recognition of pathogens (49,50). TLR7 was not expressed in human JJ012 cell line at all, but all the other TLR groups were present. No changes in the expression of TLR10 were observed with PRP-1, although sometimes it was reported that in certain cases TLR10 is able to homodimerize or heterodimerize with TLR1 and TLR2, but its ligand remains unknown (19). We have demonstrated that PRP-1 upregulates the expression of adaptor protein TICAM2 (TRAM) but not of TICAM1 (TRIF). Most TLRs share a common signaling pathway in which myeloid differentiation factor 88 (MyD88) plays a central role (51). It is known also that TLR2 can be TRAM dependent in addition to the MyD88-dependent pathway with certain MyD88 independent exceptions (51). TLR2 is also internalized following ligand binding, but in this case, MyD88-dependent signaling continues from an intracellular location away from the plasma membrane and stimulates type I IFN production through an as yet unknown mechanism (52). Due to the importance of TLR signaling in tumorigenesis, TLR agonists have potential for antitumor therapy (53-57). Both TLR and mucins have important role in host defense mechanism, however, the link between two of them in non-infectious conditions and cancer pathology deserves attention. Understanding connecting crosstalk between two of them will open new avenues for therapeutic intervention. Cancer cells might use the TLR signaling pathways much in the same way to upregulate the expression of MUCs which in turn may also regulate TLR signaling (22). Mucins are a class of major differentially expressed proteins between normal and cancer cells, which makes them a potential target for anticancer therapies. As a class of glycoproteins, MUCs are recognized as potential markers of disease progression or inhibition (58) and are currently investigated as therapeutic targets for cancer (59). Our experimental results indicated the nuclear localization of both MUC5B and TLR1/2. Indeed the evidence of their nuclear translocation was reported in the literature (24,60). Due to the importance of TLR signaling in tumorigenesis, TLR agonists have potential for antitumor therapy (22,54-58).The fact that PRP-1 has receptors of innate immunity explains observed antibacterial properties of PRP (61). The biochemical evidence for the direct interaction of TLRs or MUC5B with endogenous stimulators is limited. There is no doubt that it is of great significance to identify those ligands and elucidate their biological functions, especially if upon their binding with the ligand, the antiproliferative effect in tumor is manifested. The western blot analysis and immunocytochemistry data indicated upregulated protein expression of TLR1, TLR6, MUC5B after the treatment with PRP-1 in JJ012 human chondrosarcoma cell line, the custom

designed RT2 qPCR primer assays proved that PRP-1 indeed has effect on expression levels of its interacting partner genes as well. However, depending on the method it showed some dose response differences. For example, in case of TLR2 the protein expression upregulation with 1 and 10 μg/ml PRP-1 was observed in dose-response manner in western blot experiments. However, the heat map and qRT-PCR ΔCt calculations proved that the highest upregulation of TLR2 expression is taking place at 1 μg/ml (>5-fold upregulation). On the gene expression level, the qRT-PCR did not report significant fold change in ΔCt for TLR1 or TLR6, whereas in western blot experiments we saw obvious upregulation of protein expression for these respective receptors after the dose response treatment with PRP-1. MUC5B on the heat map demonstrated the most upregulation after the treatment with 1 μg/ml, which coincided with MUC5B ELISA results, though TriCEPS technology detected MUC5B as binding partner with 10 μg/ml PRP-1 treatment. c-Myc results demonstrated downregulation of its gene expression in dose-response manner with PRP-1, being downregulated very strongly at 10 μg/ml, which is concordant with our previous results (10). Despite these differences, it is important to mention that most of inhibitory responses caused by PRP-1 treatment on cell growth of tumor cell lines or upregulation of tumor suppressors and downregulation of oncoproteins, were maximally observed when treated with 1-20 μg/ml PRP-1 range. PRP-1 is a compound naturally produced in the body and the fact it was detected in the nucleus of chondrosarcoma cells and that it upregulated TLR1/2 dimer and TLR6 possibly indicates PRP-1 as an endogenous ligand.

The ability of TLRs to recognize endogenous stimulators appears to be essential to their function in regulating non-infectious (sterile) inflammation. TLR-induced innate immune responses regulate non-infectious sterile inflammation and subsequently, adaptive immune response. The endogenous TLR ligands and their receptors can be localized in different cellular compartments and cannot interact physiologically. However, when the tissue is injured, the passive release of endogenous ligand or its active transport utilizing non-conventional lysosomal route. In the present study, we were able to identify the pattern recognition receptors of adaptive immunity TLR1, TLR2 and TLR6, and secreted mucin MUC5B as binding partners for cytostatic PRP-1 peptide. The mentioned results allow to understand the immunomodulatory, antibacterial effect of PRP-1, reported by our group before (3,42,61). From oncologic standpoint it is important information that immune receptors play antitumorigenic role when bound to PRP-1 ligand.

Acknowledgements

References

1. Ozaki T, Hillmann A, Lindner N, Blasius S and Winkelmann W: Metastasis of chondrosarcoma. J Cancer Res Clin Oncol 122: 625-628, 1996.
2. Mirra J: Bone Tumors: Clinical, radiologic, and pathologic correlations. Lea and Febiger, Philadelphia, PA, 1989.
3. Galoyan A: Neurochemistry of brain neuroendocrine immune system: Signal molecules. Neurochem Res 25: 1343-1355, 2000.
4. Galoian K, Temple TH and Galoyan A: Cytostatic effect of the hypothalamic cytokine PRP-1 is mediated by mTOR and cMyc inhibition in high grade chondrosarcoma. Neurochem Res 36: 812-818, 2011.
5. Galoian K, Temple HT and Galoyan A: mTORC1 inhibition and ECM-cell adhesion-independent drug resistance via PI3K-AKT and PI3K-RAS-MAPK feedback loops. Tumour Biol 33: 885-890, 2012.
6. Galoian KA, Temple TH and Galoyan A: Cytostatic effect of novel mTOR inhibitor, PRP-1 (galarmin) in MDA 231 (ER-) breast carcinoma cell line. PRP-1 inhibits mesenchymal tumors. Tumour Biol 32: 745-751, 2011.
7. Galoian KA, Guettouche T, Issac B, Qureshi A and Temple HT: Regulation of onco and tumor suppressor MiRNAs by mTORC1 inhibitor PRP-1 in human chondrosarcoma. Tumour Biol 35: 2335-2341, 2014.
8. Galoian K, Qureshi A, Wideroff G and Temple HT: Restoration of desmosomal junction protein expression and inhibition of H3K9-specific histone demethylase activity by cytostatic proline-rich polypeptide-1 leads to suppression of tumorigenic potential in human chondrosarcoma cells. Mol Clin Oncol 3: 171-178, 2015.
9. Galoian K, Luo S, Qureshi A, Patel P, Price R, Morse AS, Chailyan G, Abrahamyan S and Temple HT: Effect of cytostatic proline rich polypeptide-1 on tumor suppressors of inflammation pathway signaling in chondrosarcoma. Mol Clin Oncol 5: 618-624, 2016.
10. Galoian K, Qureshi A, D'Ippolito G, Schiller PC, Molinari M, Johnstone AL, Brothers SP, Paz AC and Temple HT: Epigenetic regulation of embryonic stem cell marker miR302C in human chondrosarcoma as determinant of antiproliferative activity of proline-rich polypeptide 1. Int J Oncol 47: 465-472, 2015.
11. Yu L, Wang L and Chen S: Exogenous or endogenous Toll-like receptor ligands: Which is the MVP in tumorigenesis? Cell Mol Life Sci 69: 935-949, 2012.
12. Rakoff-Nahoum S and Medzhitov R: Toll-like receptors and cancer. Nat Rev Cancer 9: 57-63, 2009.
13. Joshi S, Kumar S, Choudhury A, Ponnusamy MP and Batra SK: Altered Mucins (MUC) trafficking in benign and malignant conditions. Oncotarget 5: 7272-7284, 2014.
14. Blasius AL and Beutler B: Intracellular toll-like receptors. Immunity 32: 305-315, 2010.
15. Huang B, Zhao J, Unkeless JC, Feng ZH and Xiong H: TLR signaling by tumor and immune cells: A double-edged sword. Oncogene 27: 218-224, 2008.
16. Apetoh L, Ghiringhelli F, Tesniere A, Obeid M, Ortiz C, Criollo A, Mignot G, Maiuri MC, Ullrich E, Saulnier P, et al: Toll-like receptor 4-dependent contribution of the immune system to anticancer chemotherapy and radiotherapy. Nat Med 13: 1050-1059, 2007.
17. Medzhitov R: Origin and physiological roles of inflammation. Nature 454: 428-435, 2008.
18. Seong SY and Matzinger P: Hydrophobicity: An ancient damage-associated molecular pattern that initiates innate immune responses. Nat Rev Immunol 4: 469-478, 2004.
19. Hasan U, Chaffois C, Gaillard C, Saulnier V, Merck E, Tancredi S, Guiet C, Brière F, Vlach J, Lebecque S, et al: Human TLR10 is a functional receptor, expressed by B cells and plasmacytoid dendritic cells, which activates gene transcription through MyD88. J Immunol 174: 2942-2950, 2005.
20. Lowe EL, Crother TR, Rabizadeh S, Hu B, Wang H, Chen S, Shimada K, Wong MH, Michelsen KS and Arditi M: Toll-like receptor 2 signaling protects mice from tumor development in a mouse model of colitis-induced cancer. PLoS One 5: e13027, 2010.
21. Yu L, Wang L and Chen S: Endogenous toll-like receptor ligands and their biological significance. J Cell Mol Med 14: 2592-2603, 2010.

22. Tarang S, Kumar S and Batra SK: Mucins and toll-like receptors: Kith and kin in infection and cancer. Cancer Lett 321: 110-119, 2012.

23. Kanzler H, Barrat FJ, Hessel EM and Coffman RL: Therapeutic targeting of innate immunity with Toll-like receptor agonists and antagonists. Nat Med 13: 552-559, 2007.

24. Lakshminarayanan V, Thompson P, Wolfert MA, Buskas T, Bradley JM, Pathangey LB, Madsen CS, Cohen PA, Gendler SJ and Boons GJ: Immune recognition of tumor-associated mucin MUC1 is achieved by a fully synthetic aberrantly glycosylated MUC1 tripartite vaccine. Proc Natl Acad Sci USA 109: 261-266, 2012.

25. Hollingsworth MA and Swanson BJ: Mucins in cancer: Protection and control of the cell surface. Nat Rev Cancer 4: 45-60, 2004.

26. Remmers N, Anderson JM, Linde EM, DiMaio DJ, Lazenby AJ, Wandall HH, Mandel U, Clausen H, Yu F and Hollingsworth MA: Aberrant expression of mucin core proteins and o-linked glycans associated with progression of pancreatic cancer. Clin Cancer Res 19: 1981-1993, 2013.

27. Sóñora C, Mazal D, Berois N, Buisine MP, Ubillos L, Varangot M, Barrios E, Carzoglio J, Aubert JP and Osinaga E: Immunohistochemical analysis of MUC5B apomucin expression in breast cancer and non-malignant breast tissues. J Histochem Cytochem 54: 289-299, 2006.

28. Kim YS, Gum J Jr and Brockhausen I: Mucin glycoproteins in neoplasia. Glycoconj J 13: 693-707, 1996.

29. Turner MS, McKolanis JR, Ramanathan RK, Whitcomb DC and Finn OJ: Mucins in gastrointestinal cancers. Cancer Chemother Biol Response Modif 21: 259-274, 2003.

30. Berois N, Varangot M, Sóñora C, Zarantonelli L, Pressa C, Laviña R, Rodríguez JL, Delgado F, Porchet N, Aubert JP, *et al*: Detection of bone marrow-disseminated breast cancer cells using an RT-PCR assay of MUC5B mRNA. Int J Cancer 103: 550-555, 2003.

31. Moniaux N, Andrianifahanana M, Brand RE and Batra SK: Multiple roles of mucins in pancreatic cancer, a lethal and challenging malignancy. Br J Cancer 91: 1633-1638, 2004.

32. Andrianifahanana M, Moniaux N and Batra SK: Regulation of mucin expression: Mechanistic aspects and implications for cancer and inflammatory diseases. Biochim Biophys Acta 1765: 189-222, 2006.

33. Kufe DW: Mucins in cancer: Function, prognosis and therapy. Nat Rev Cancer 9: 874-885, 2009.

34. Velcich A, Yang W, Heyer J, Fragale A, Nicholas C, Viani S, Kucherlapati R, Lipkin M, Yang K and Augenlicht L: Colorectal cancer in mice genetically deficient in the mucin Muc2. Science 295: 1726-1729, 2002.

35. Van Seuningen I, Perrais M, Pigny P, Porchet N and Aubert JP: Sequence of the 5'-flanking region and promoter activity of the human mucin gene MUC5B in different phenotypes of colon cancer cells. Biochem J 348: 675-686, 2000.

36. Aziz MA, AlOtaibi M, AlAbdulrahman A, AlDrees M and AlAbdulkarim I: Mucin family genes are downregulated in colorectal cancer patients. J Carcinogene Mutagene S10:009. 2014.

37. Wakata K, Tsuchiya T, Tomoshige K, Takagi K, Yamasaki N, Matsumoto K, Miyazaki T, Nanashima A, Whitsett JA, Maeda Y, *et al*: A favourable prognostic marker for EGFR mutant non-small cell lung cancer: Immunohistochemical analysis of MUC5B. BMJ Open 5: e008366, 2015.

38. Roy MG, Livraghi-Butrico A, Fletcher AA, McElwee MM, Evans SE, Boerner RM, Alexander SN, Bellinghausen LK, Song AS, Petrova YM, *et al*: Muc5b is required for airway defence. Nature 505: 412-416, 2014.

39. Vincent A, Perrais M, Desseyn JL, Aubert JP, Pigny P and Van Seuningen I: Epigenetic regulation (DNA methylation, histone modifications) of the 11p15 mucin genes (MUC2, MUC5AC, MUC5B, MUC6) in epithelial cancer cells. Oncogene 26: 6566-6576, 2007.

40. Macha MA, Krishn SR, Jahan R, Banerjee K, Batra SK and Jain M: Emerging potential of natural products for targeting mucins for therapy against inflammation and cancer. Cancer Treat Rev 41: 277-288, 2015.

41. Markossian KA, Gurvits BY and Galoyan AA: Isolation and identification of novel peptides from secretory granules of neurohypophysis. Neurochem Res 16: 22, 1999.

42. Galoyan AA: Brain neurosecretory cytokines: immune response and neuronal survival. Kluwer Academic Plenum Publishers, New York, 2004. https://doi.org/10.1007/978-1-4419-8893-5.

43. Abrahamyan SS, Davtyan TK, Khachatryan AR, Tumasyan NV, Sahakyan IK, Harutyunyan HA, Chailyan SG and Galoyan AA: Quantification of the hypothalamic proline rich polypeptide-1 in rat blood serum. Neurochem J 8: 38-43, 2014.

44. Yan YX, Boldt-Houle DM, Tillotson BP, Gee MA, D'Eon BJ, Chang XJ, Olesen CE and Palmer MA: Cell-based high-throughput screening assay system for monitoring G protein-coupled receptor activation using beta-galactosidase enzyme complementation technology. J Biomol Screen 7: 451-459, 2002.

45. Frei AP, Moest H, Novy K and Wollscheid B: Ligand-based receptor identification on living cells and tissues using TRICEPS. Nat Protoc 8: 1321-1336, 2013.

46. Slavoff SA and Saghatelian A: Discovering ligand-receptor interactions. Nat Biotechnol 30: 959-961, 2012.

47. Omasits U, Ahrens CH, Müller S and Wollscheid B: Protter: Interactive protein feature visualization and integration with experimental proteomic data. Bioinformatics 30: 884-886, 2014.

48. Senapati S, Das S and Batra SK: Mucin-interacting proteins: From function to therapeutics. Trends Biochem Sci 35: 236-245, 2010.

49. Ozinsky A, Underhill DM, Fontenot JD, Hajjar AM, Smith KD, Wilson CB, Schroeder L and Aderem A: The repertoire for pattern recognition of pathogens by the innate immune system is defined by cooperation between toll-like receptors. Proc Natl Acad Sci USA 97: 13766-13771, 2000.

50. Janssens S and Beyaert R: Role of Toll-like receptors in pathogen recognition. Clin Microbiol Rev 16: 637-646, 2003.

51. Nilsen N, Nonstad U, Khan N, Knetter CF, Akira S, Sundan A, Espevik T and Lien E: Lipopolysaccharide and double-stranded RNA up-regulate toll-like receptor 2 independently of myeloid differentiation factor 88. J Biol Chem 279: 39727-39735, 2004.

52. Seibert SA, Mex P, Köhler A, Kaufmann SH and Mittrücker HW: TLR2-, TLR4- and Myd88-independent acquired humoral and cellular immunity against Salmonella enterica serovar Typhimurium. Immunol Lett 127: 126-134, 2010.

53. Jeung HC, Moon YW, Rha SY, Yoo NC, Roh JK, Noh SH, Min JS, Kim BS and Chung HC: Phase III trial of adjuvant 5-fluorouracil and adriamycin versus 5-fluorouracil, adriamycin, and polyadenylic-polyuridylic acid (poly A:U) for locally advanced gastric cancer after curative surgery: final results of 15-year follow-up. Ann Oncol 19: 520-526, 2008.

54. Smits EL, Ponsaerts P, Berneman ZN and Van Tendeloo VF: The use of TLR7 and TLR8 ligands for the enhancement of cancer immunotherapy. Oncologist 13: 859-875, 2008.

55. Leonard JP, Link BK, Emmanouilides C, Gregory SA, Weisdorf D, Andrey J, Hainsworth J, Sparano JA, Tsai DE, Horning S, *et al*: Phase I trial of toll-like receptor 9 agonist PF-3512676 with and following rituximab in patients with recurrent indolent and aggressive non Hodgkin's lymphoma. Clin Cancer Res 13: 6168-6174, 2007.

56. Mikulandra M, Pavelic J and Glavan TM: Recent findings on the application of Toll-like receptors agonists in cancer therapy. Curr Med Chem 24: 2011-2032, 2017.

57. Kaczanowska S, Joseph AM and Davila E: TLR agonists: Our best frenemy in cancer immunotherapy. J Leukoc Biol 93: 847-863, 2013.

58. Rachagani S, Torres MP, Moniaux N and Batra SK: Current status of mucins in the diagnosis and therapy of cancer. Biofactors 35: 509-527, 2009.

59. Planque N: Nuclear trafficking of secreted factors and cell-surface receptors: New pathways to regulate cell proliferation and differentiation, and involvement in cancers. Cell Commun Signal 4: 7, 2006.

60. Huhta H, Helminen O, Lehenkari PP, Saarnio J, Karttunen TJ and Kauppila JH: Toll-like receptors 1, 2, 4 and 6 in esophageal epithelium, Barrett's esophagus, dysplasia and adenocarcinoma. Oncotarget 7: 23658-23667, 2016.

61. Galoyan AA: Brain immune system signal molecules in protection from aerobic and anaerobic infections. In: Advances in Neurobiology. Vol 6: Springer, 2012.